Solubility Measurements of N_2 and CO_2 in Polypropylene and Ethene/Octene Copolymer

G. Li,[1] F. Gunkel,[2] J. Wang,[2] C. B. Park,[1] V. Altstädt[2]

[1]Department of Mechanical & Industrial Engineering, University of Toronto, Toronto M5S 3G8, Canada
[2]Polymer Engineering, University of Bayreuth, Universitätsstr. 30, D-95447 Bayreuth, Germany

ABSTRACT: In this set of experiments a magnetic suspension balance (MSB) was employed to measure the apparent solubilities of N_2 and CO_2 in polypropylene (PP) and ethene/octene copolymer melts, while the swollen volume predicted by the Sanchez–Lacombe (SL) equation of state (EOS) was used to account for the buoyancy effect. The swollen volume of the polymer/gas mixture, as well as the gas solubilities for both PP and the ethene/octene copolymer, are discussed. It was observed that the branched molecular structure limited the molecular movement, and therefore the volume swelling of the polymer/gas mixture. In a similar context, the solubility of both N_2 and CO_2 were less in the branched polymer (ethene/octene copolymer) than in the linear PP. © 2006 Wiley Periodicals, Inc. J Appl Polym Sci 103: 2945–2953, 2007

Key words: solubility; magnetic suspension balance; polypropylene; ethene/octene copolymer; Henry's constants; nitrogen; carbon dioxide

INTRODUCTION

Determining the solubility of blowing agents, such as supercritical N_2 and CO_2, in polypropylene (PP) and elastomeric materials is crucial for manufacturing high quality thermoplastic polyolefin (TPO) foams. Thermoplastic polyolefins (TPOs) are polymer blend systems with a continuous plastic matrix and a dispersed rubbery phase.[1,2] With their improved impact resistance, balanced physical and mechanical properties,[3] recyclability, excellent processibility, and low cost, the TPOs find lots of potential applications in the automotive industry. Among the vast number of plastic automobile parts, the TPO bumper constitutes the largest market share. As such, the successful completion of the development of TPO foaming technology will result in a significant savings of material costs, which will be a huge benefit to the automobile makers. It should be noted that while some research has already been conducted on TPO foaming technology with the aim of developing it for the automobile industry,[4] additional studies are still required. For example, since TPO injection-foaming is integral to the innovative manufacturing technique of bumper fascia and is an environmentally benign technology that uses supercritical nitrogen, the refinement of this technique represents an essential step in broadening its applications for a new generation of vehicle parts production. The main plastic component in TPO materials is PP, which is quite useful in industrial applications due to its advantageous mechanical properties and high service temperature range.[5] Ethene/octene polyolefin copolymer elastomer has become the modifier of choice for automotive TPO applications; ethene/octene rubber is increasingly preferred for all polyolefin auto interior components and innovative interiors designs.

Plastic foams are usually formed by using blowing agents, such as volatile liquids, supercritical gases, or chemical compounds, which generate gases during the foaming process.[6,7] Typically, plastic foams are created by exposing the polymer/gas mixture system to thermodynamic instability to obtain a high number of nucleation sites, and therefore, a high cell density in the polymer matrix once the polymer/gas single-phase solution has been formed.[8] Plastic foams processing involves the following steps: (a) polymer/gas single-phase solution formation; (b) bubble nucleation; (c) bubble growth; and (d) foam structure stabilization. The formation of a polymer/gas single-phase solution is accomplished by dissolving a gas, such as CO_2 or N_2, into a polymer melt under high temperature and pressure. The polymer/gas solution is then subjected to the thermodynamic instability in order for bubble nucleation to proceed. The thermodynamic instability is achieved by rapidly lowering the gas solubility in the polymer via a temperature increase and/or a pressure drop. Therefore, the solubility of

the blowing agent introduced into the polymer melt is a critical factor[6,9] in plastic foam processing as it directly affects all foaming behaviors. Gaining additional knowledge about gas solubilities will not only help researchers and manufacturers determine the maximum amount of gas that can be injected into a given polymer melt, but will also impact the kinetic process of foaming (i.e., nucleation; the cell nucleation mechanism has been described in detail in previous studies[10–12]). Furthermore, to obtain cellular plastic foams that exhibit large volume expansion during continuous processing, the processing temperature must be reduced to prevent cell coalescence and to preserve high cell density.[13,14] These pressure and temperature changes affect the solubility of the gas in the polymer, and thus influence the cellular morphology of the foam (i.e., the cell density, expansion ratio, and open cell content).[12–14] Therefore, solubility has always been, and remains to be, of great interest to foaming manufacturers and researchers. This research investigates the solubilities of N_2 and CO_2 in the two main components in TPO materials, i.e., PP and ethene/octene polyolefin copolymer elastomer.

Theory and background

Because of the substantial interest in the solubility of blowing agents in polymers during the foaming process, many efforts have been made to study the solubility from both the experimental and theoretical aspects. Sato et al.[15,16] have investigated the solubilities of CO_2 and N_2 in PS, PP, and HDPE using a pressure decay approach. They also have extensively measured the solubilities of CO_2 and N_2 in PS, PVAC, PBS, and PPO/PS blends with a magnetic suspension balance (MSB),[17–19] while Areerat et al. have utilized the MSB to evaluate the solubility of CO_2 in LDPE.[20] Wong et al.[21] explored the solubility of CO_2 in PS and PVC using an electrobalance. In addition to the variety of experimental methods employed to achieve solubility measurements, various approaches have been applied to account for the buoyancy effect produced by the swollen volume of the polymer/gas mixture. Most researchers have used the Sanchez–Lacombe (SL) equation of state (EOS),[15,17–20] while Wong et al.[21] have applied the partial volume theory to predict the swollen volume caused by the dissolution of gas in the polymer. Sato et al.[17–19] had done a thorough study on the volume swelling of polymer/gas mixtures based on the SL EOS for the buoyancy effect compensation to get reliable solubility data. Recently, Simha–Somcynsky (SS) EOS was used by Li et al. to predict the PVT behavior of the polymer/gas mixture as well; they also performed a comparison between their results and the results obtained in experiments that used SL EOS.[22]

The MSB and SL EOS were applied in this study. Interested readers may refer to our previous paper for a detailed outline of this methodology.[22] In summary, EOS was employed to predict the PVT behavior for the polymer/gas mixture, as well as to calculate the theoretical solubility. The specific volume of the polymer/gas mixture, $v_{p,\text{mixture}}$ (cm^{-3}/g), can be calculated at certain conditions (composition, temperature, and pressure) by solving the SL EOS.[23,24] Then the swollen volume, V_s, can easily be calculated using eq. (1):

$$V_s = \left[(1 + S) \times v_{p,\text{mixture}} - v_{p,\text{pure polymer}} \right] \times m \quad (1)$$

where S is the theoretical gas solubility (g-gas/g-polymer) in the polymer melt; m is the initial weight of the polymer sample (g); $v_{p,\text{pure polymer}}$ (cm^{-3}/g) is the specific volume of the pure polymer; and $v_{p,\text{mixture}}$ (cm^{-3}/g) is the specific volume of the polymer/gas mixture. The volume swelling ratio (S_w), which is defined in eq. (2), describes the swelling effect due to the gas dissolution in the polymer melt.

$$S_w = \frac{(1 + S) \times v_{p,\text{mixture}}}{v_{p,\text{pure polymer}}} \quad (2)$$

EXPERIMENTAL

Materials and characterization

Linear PP (DM 55, Borealis, Austria), ethene/octene copolymer (Engage[TM] 8407, monomer ratio: ethene/octene 60/40 wt %, Dow), carbon dioxide (Coleman grade, 99.99% purity, BOC Canada), nitrogen (BOC Canada), and all other materials were used as received.

PVT data for PP and ethene/octene copolymer

The moldflow equation [see eq. (3)] for linear PP was derived from the PVT data of linear PP, which was measured at Datapointlabs (Ithaca, NY) using a Gnomix PVT apparatus. These PVT data of the pure linear PP are also used to derive the corresponding characteristic parameters in SL-EOS: P^*, V^*, T^* shown in Table I.

$$v_p = \left(\frac{7.46 \times 10^6}{6.45 \times 10^9 + P} + \frac{1.06 \times 10^2 \times T}{9.86 \times 10^7 + P} \right) \times 1000 \quad (3)$$

In the above equation, the temperature T is in (°C) and pressure P is in (Pa).

In Suhm's study, the PVT data were measured for various ethene/octene copolymers that exhibited different monomer ratios.[25] We chose to use the PVT data for E-co-O-39 in this study to ensure that Engage 8407 and E-co-O-39 have the same monomer ratio. Therefore, based on the published PVT data of ethene/octene copolymer from Suhm's measure-

TABLE I
Scaling Parameters for SL EOS

Substance	P^* (MPa)	V^* (cm^3/g)	T^* (K)	Reference
Linear PP	312.2	1.1563	679.5	This work
Ethene/octene copolymer	359.3	1.1132	649.9	This work
CO$_2$	720.3	0.6329	$208.9 + 0.459\,T - 7.56 \times 10^{-4}\,T^2$	Ref. 17
N$_2$	103.6	1.2447	159.0	Ref. 22

ment,[25] the Tait equation for ethene/octene copolymer, i.e., eq. (4), was derived.

$$v_p = 1.1185 e^{(8.9671 \times 10^{-4} T)}$$
$$\times \left(1 - 0.0891 \ln\left(1 + \frac{P}{2289 \times e^{(-6.8909 \times 10^{-3} T)}}\right)\right) \quad (4)$$

In the above equation, the temperature T is in (°C) and pressure P is in (Bar).

Furthermore, the PVT data of ethene/octene copolymer[25] was used to derive the corresponding SL-EOS characteristic parameters for ethene/octene copolymer: P^*, V^*, and T^*, which are listed in Table I.

Apparatus used for solubility measurements and experimental procedures

The sorption isotherms of N$_2$ and CO$_2$ in PP and ethene/octene copolymer melts were determined gravimetrically using an MSB[26] from Rubotherm GmbH. The schematic of MSB was illustrated in Figure 1. (A more detailed description of the experimental apparatus and procedures for use are available in a previous publication.[22])

In brief, a precisely weighted sample was carefully placed in the sample container inside the sorption chamber prior to commencing the sorption experi-

ment. The chamber was then sealed, evacuated, and preheated to a designated temperature. The high-pressure gas was then introduced into the sorption chamber; the gas pressure inside the chamber was maintained at a desired value by a syringe pump (260D, ISCO). Throughout the course of the sorption process, a Julabo TD-6 Heating Circulator was utilized to control the temperature with precision. Because of the dissolution of gas in the polymer sample, the total weight of the sample kept increasing. When the saturation or the equilibrium condition was reached, the weight of the sample did not increase any more and remained stabilized. The balance read-out at vacuum and temperature (T) was recorded as $W(0,T)$. The balance weight read-out at each equilibrium condition was determined at the corresponding pressures (P) and temperatures (T), and was recorded as $W(P,T)$. Hence, the amount of gas dissolved in the polymer at each specific condition (P, T), W_g, was calculated by employing eq. (5):[22]

$$W_g = W(P,T) - W(0,T) + \rho(V_B + V_P + V_S) \quad (5)$$

where ρ is the density of gas; V_B is the volume of the sample holder; V_P is the volume of the pure polymer sample at pressure P and temperature T; and V_S is the total swollen volume of the sample caused by gas dis-
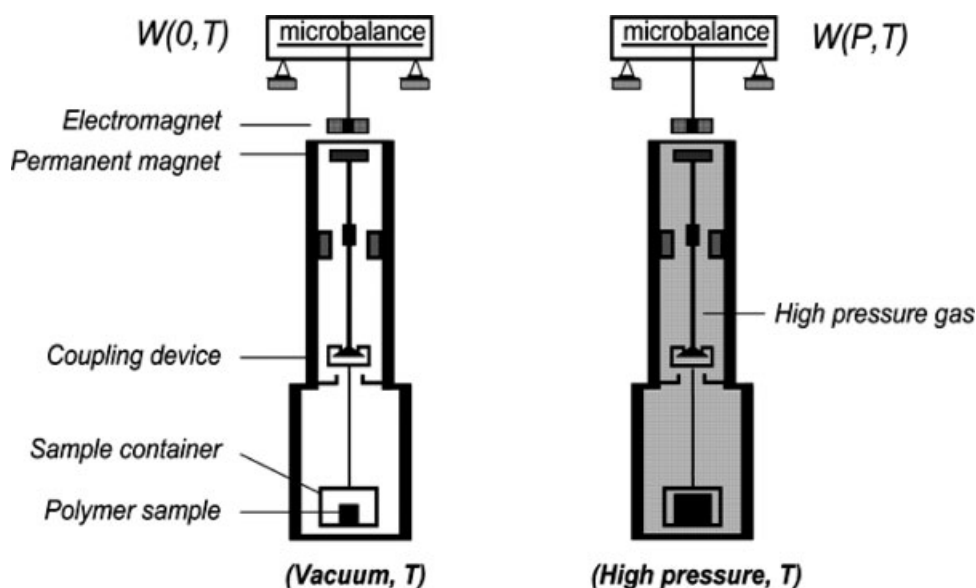

Figure 1 Schematic of magnetic suspension balance.

solution. During gas dissolution, the total volume of the polymer/gas mixture increased. SL EOS was applied to predict the total swollen volume ratio of the polymer/gas mixture at equilibrium conditions as described above in eq. (1).

By ignoring the polymer swollen volume term (V_S) in eq. (5), the measured weight gain was treated as the apparent weight gain, $W_{g, \text{apparent}}$ [eq. (6)]:

$$W_{g,\text{apparent}} = W(P,T) - W(0,T) + \rho(V_B + V_P) \quad (6)$$

The apparent solubility (X_{apparent}) and the corrected solubility ($X_{\text{corrected}}$) can therefore be calculated using eqs. (7) and (8), respectively:

$$X_{\text{apparent}} = W_{g,\text{apparent}}/\text{Mass of Sample} \quad (7)$$

$$X_{\text{corrected}} = X_{\text{apparent}} + (\rho \times V_s)/\text{Mass of Sample} \quad (8)$$

RESULTS AND DISCUSSION

Specific volume of pure polymers and polymer/gas mixtures

The specific volumes of the pure polymer melts (ethene/octene copolymer and PP) were determined using either the Tait equation [eq. (4)] or the moldflow equation [eq. (3)], while the specific volumes of the polymer/gas mixtures were calculated using SL EOS. All specific volumes of pure polymer and polymer/gas mixture in dependency on temperature and pressure are listed in Figures 2 and 3. As shown in Figure 2, the pure polymer melts (ethene/octene copolymer and PP) demonstrated similarities concerning their thermal expansion and pressure compressibility as the results indicate. With increasing pressure and decreasing temperature, the specific volumes of the pure polymers decrease, which is believed to be caused by a reduction of the free volume. The only no-
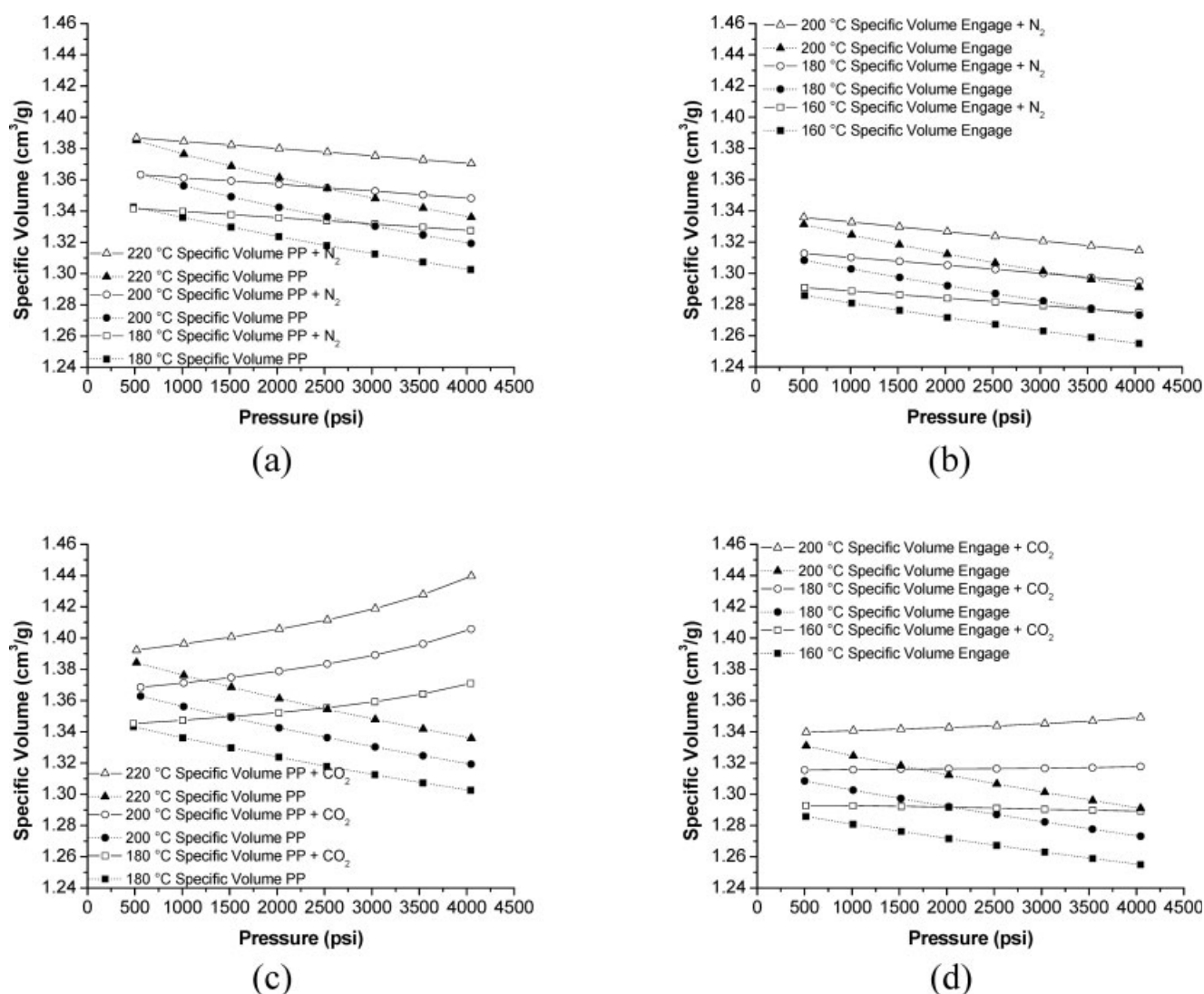

Figure 2 Specific volume of mixture of (a) PP + N_2; (b) ethene/octene copolymer + N_2; (c) PP + CO_2; and (d) ethene/octene copolymer + CO_2.
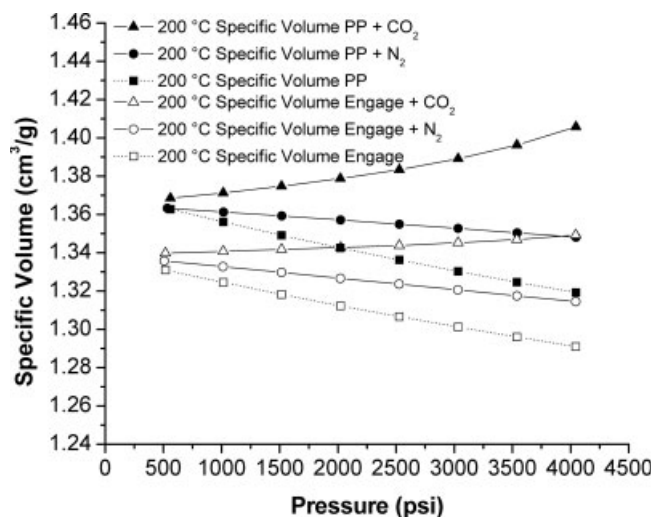
Figure 3 Comparison of specific volumes.

ticeable difference between ethene/octene copolymer and PP lies in the absolute value, as the PP turns out having a higher specific volume than the ethene/octene copolymer.

Throughout the experiments, the specific volumes of the polymer/gas mixtures exceed those of the corresponding neat polymer melts. Being greater than those of the pure melts, the specific volumes of the polymer/N$_2$ mixtures still show a negative compressibility coefficient with respect to pressure. In contrast to that, the specific volumes of the polymer/CO$_2$ mixtures increase with pressure as shown in Figure 3. It is believed that there are several reasons contributing to the fact of specific volume change of a polymer/CO$_2$ mixture during the gas dissolution process, such as the plain mixture of the components (gas molecules and polymer chain molecules), as well as the change of the free volume. On the one hand, with the introduction of high pressure CO$_2$, the hydraulic pressure reduces the amount of free volume (unoccupied volume) in the lattice structure of the polymer melt and therefore decreases the specific volume (the compressibility of polymer melts); on the other hand, the high pressure CO$_2$ causes a polymer/CO$_2$ solution and therefore affects the free volume. The dissolved gas as such can reduce the original amount of free volume by occupying it, but may then again generate a certain amount of free volume itself since there are more unoccupied sites associated with gas lattice structure and therefore the dissolution of gas in a polymer melt implies the introduction of occupied volume (gas molecules), together with unoccupied volume (free volume) as well, into the lattice structure of the polymer melt. Hence, applying higher gas pressures, and therefore dissolving more gas into the polymer, may eventually generate more free volume in the polymer/gas solution, thus decreasing the overall specific volume.

Figure 3 compares the mixtures with respect to the polymer component. One can observe a greater increase of specific volume due to gas dissolution in PP than in the ethene/octene copolymer. It is believed that the branched structure of the copolymer is less favorable for the gas to dissolve and therefore allowing less free volume to be generated, resulting in lower specific volumes than the comparable linear PP.

Volume swelling of the polymer/gas mixtures

Based on the specific volume information obtained above, the volume swelling ratios of the polymer/gas mixtures were determined for both materials (ethene/octene copolymer and PP) with dissolved N$_2$ and CO$_2$, respectively, (the results are listed in Figs. 4 and 5). One can observe that each mixture shows an increase of the swelling ratio with increasing pressure. Regarding Figure 4, one can observe higher swelling ratios of the polymer/N$_2$ mixtures occurring as the temperature increases, whereas the volume swelling of the polymer/CO$_2$ mixtures does not show sensitivity to temperature much.

The biggest impact on the swelling ratio was observed while comparing the mixtures with respect to the dissolved gas. The total volume swelling ratios of the polymer/N$_2$ mixtures do not exceed 1.07, whereas dissolved CO$_2$ in the copolymer and PP induces swelling ratios that amount up to 1.3 and 1.4, respectively. It is believed that the large amount of dissolved CO$_2$ in polymer melts accounted for the swollen volume primarily. Moreover, an increasing specific volume of the polymer/CO$_2$ mixtures with increasing pressure immediately implicates an even a higher increase of the volume swelling ratio according to eq. (2); therefore the observed phenomenon becomes clear.

The linear PP shows a higher volume swelling compared with the random branched ethene/octene copolymer at each corresponding temperature with N$_2$ and CO$_2$, respectively. This trend apparently shows analogy to the effect of polymer on the specific volume of the mixtures.

N$_2$ and CO$_2$ solubility

For the purpose of solubility measurements, in general it is essential that the volume swelling data be obtained after the apparent solubility has been measured using an MSB. The volume swelling predictions yielded from the SL EOS were adapted to compensate for the effects of buoyancy on the apparent solubility, as illustrated in eq. (8). In Figures 6 and 7, the solubilities of N$_2$ and CO$_2$ in the ethene/octene copolymer and PP, respectively, are represented. Throughout the experimental proceeding, it was noticeable that CO$_2$ has a much higher solubility in both polymers than
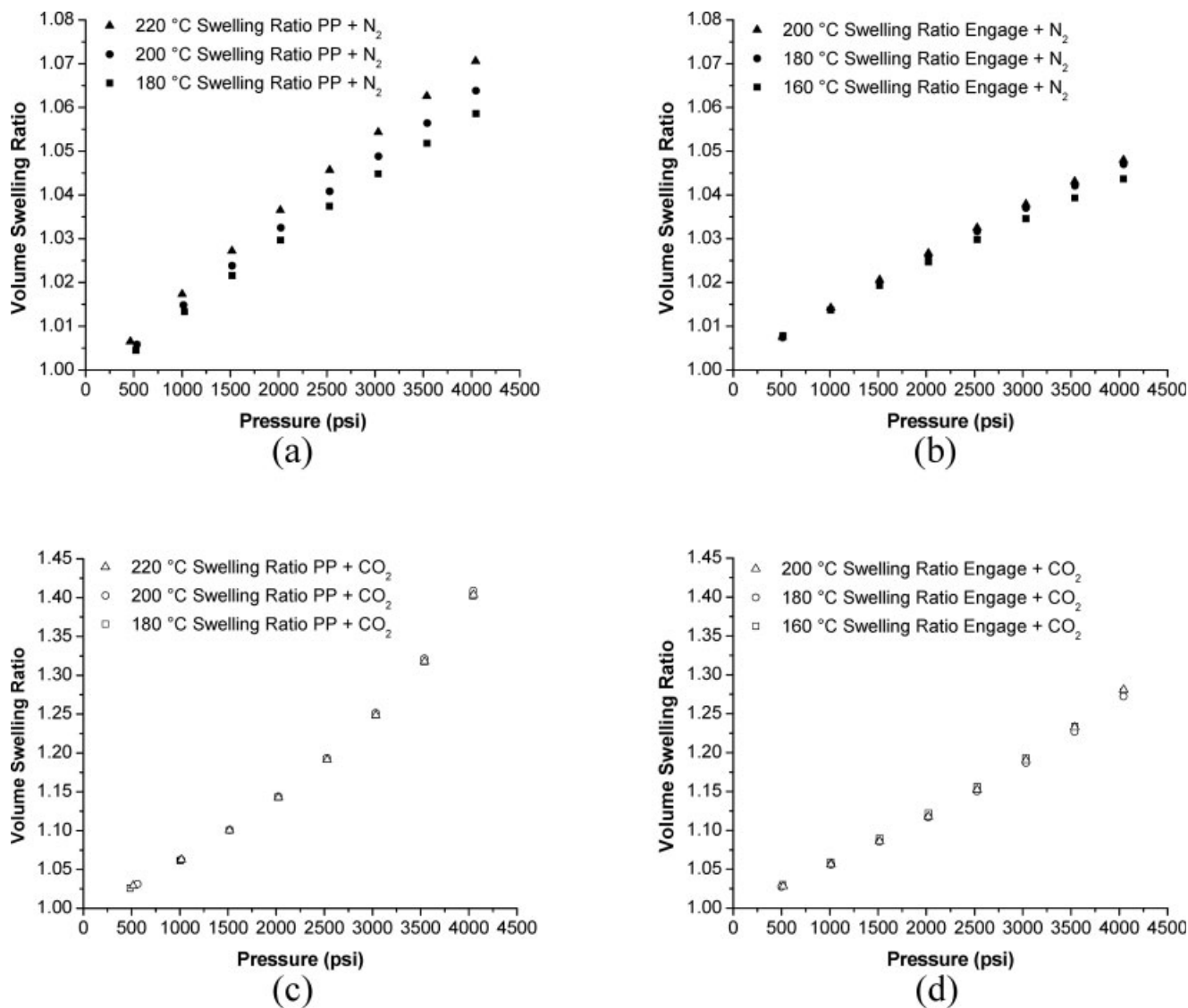
Figure 4 Volume swelling ratio of polymer/gas mixtures (a) PP + N$_2$; (b) ethene/octene copolymer + N$_2$; (c) PP + CO$_2$; and (d) ethene/octene copolymer + CO$_2$.

N$_2$. The results show a difference in approximately one order of magnitude for the solubility of CO$_2$; this becomes obvious in Figure 7. The fact that the solubility of CO$_2$, in both polymers, outruns that of N$_2$ by approximately one order of magnitude is assumed to be the reason for the dramatically increasing specific volume of mixture at elevated pressures.

In all cases significant differences between the corrected and the apparent solubility were observed as pressure exceeds 1000 psi, which is shown in Figure 6. It is easily understood that the deviations between the corrected and the apparent solubility is significant due to both the bigger amount of swollen volume (V$_s$), and higher gas density at pressures above 1000 psi. Being induced by buoyancy effects and therefore by the volume swelling of the samples, deviations of corrected and apparent solubilities of CO$_2$ are greater than those of N$_2$ because of the higher amount of vol-
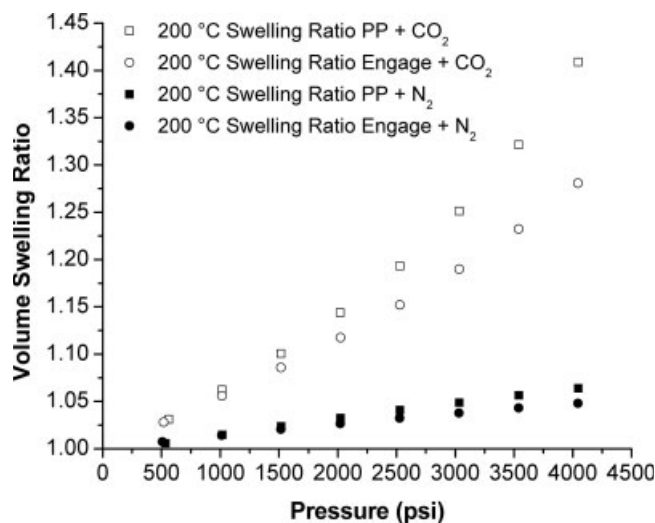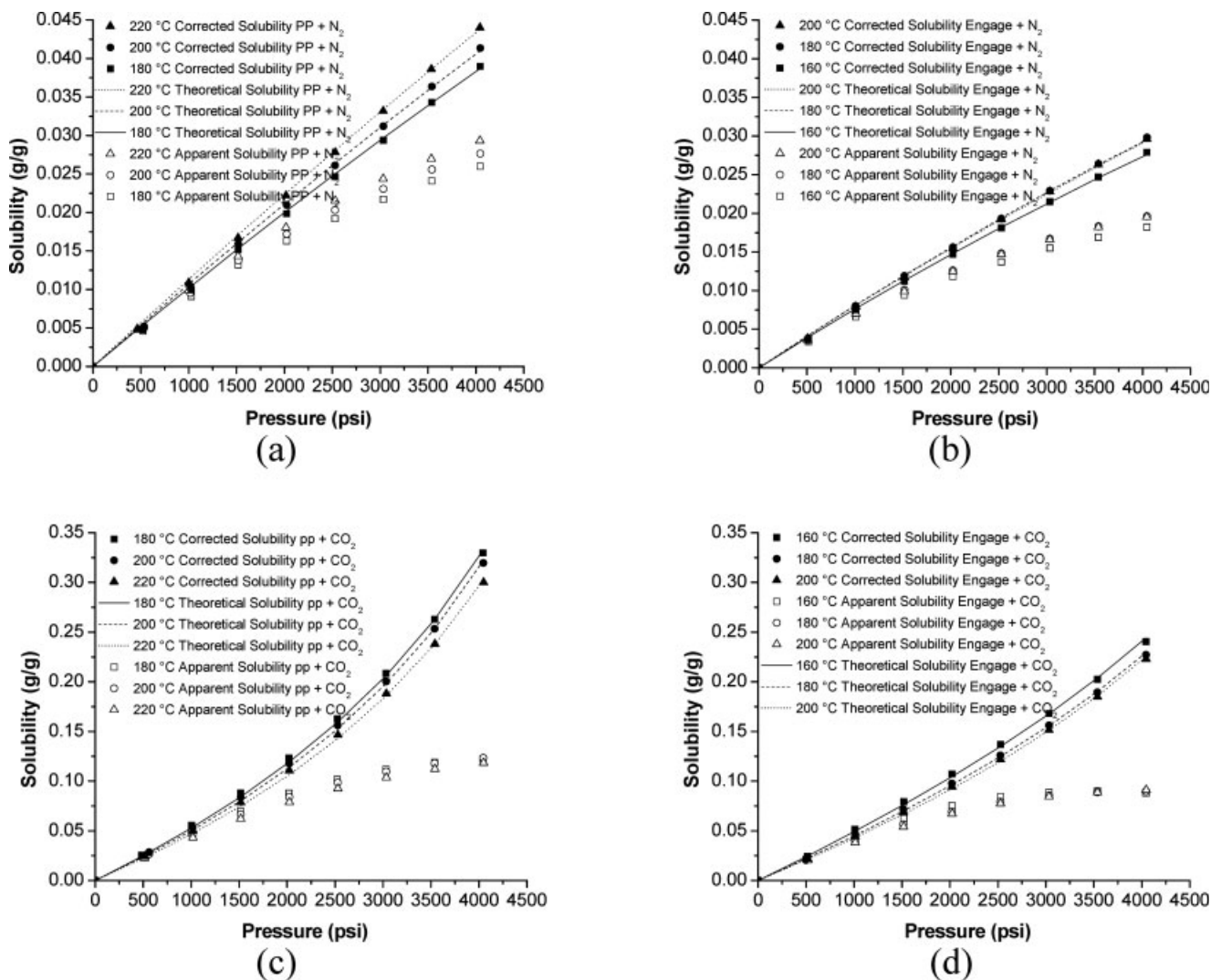

Figure 5 Comparison of volume swelling ratios.

Figure 6 Solubility of gas in polymer melts (a) PP + N$_2$; (b) ethene/octene copolymer + N$_2$; (c) PP + CO$_2$; and (d) ethene/octene copolymer + CO$_2$.

ume swelling (see Figs. 4 and 5). Each mixture system shows an increase of solubility with increasing pressure. The effect of temperature on solubility however, depends on the blowing agent. An increase of temperature would result in higher solubilities as far as N$_2$ is concerned, whereas the solubility of CO$_2$ would decrease with increasing temperature for both polymers (Fig. 6). This reverse effect of temperature is caused by the nature of gas dissolution into the polymer, which is totally opposite for CO$_2$ and N$_2$ in terms of their heat of dissolution.

Another effect on the solubility is noticeable with respect to the used polymer. Both gases demonstrate consistently higher solubilities in PP than in the copolymer material, which is caused by the different molecular structures of the two polymers. The copolymer has relatively long random branches along the C—C backbone chain, whereas the used PP is prevailingly
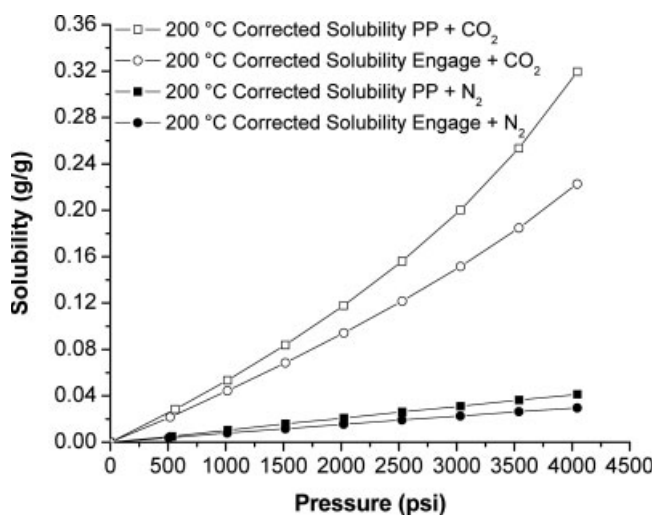

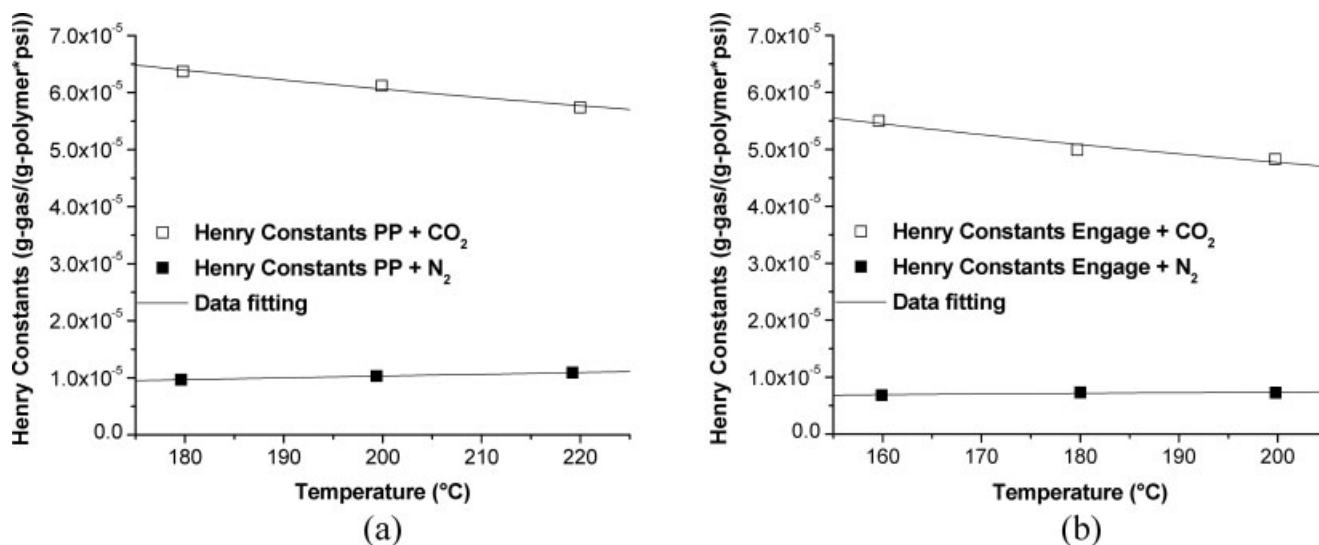**Figure 7** Comparison of gas solubilities.

Figure 8 Henry's constants of gases in (a) PP and (b) ethene/octene copolymer.

linear. It is believed that the entanglements among the molecular chains caused by the branches generate a high resistance to volume expansion and therefore create less accommodation for the gas molecules than do the linear PP chains. The enhancement of solubility by linear polymer chains has been reported in other researches as well.[27]

Henry's constants

The Henry's constants $H_p(T)$ have been determined from the experimentally obtained solubility information for each polymer/gas mixture. Based on the experimental $H_p(T)$, the equation describing the dependency of Henry's constant on temperature was derived. In general the Henry's constants are given by eq. (9):

$$H_p(T) = H_0 \exp\left(-\frac{E_a}{RT}\right) \qquad (9)$$

Figure 8 shows the experimental Henry's constants as well as plots of eq. (9) for each case. The used parameters for eq. (9) are listed in Table II.

Summary

This paper investigated the solubilities of N_2 and CO_2 in the melts of PP and the polyolefin elastomer (ethene/octene copolymer) at temperatures of 180°C, 200°C, and 220°C for PP and 160°C, 180°C, and 200°C for ethene/octene copolymer respectively. The applied pressures ranged upto 4000 psi. A MSB was used to obtain the apparent solubilities, whereas the SL EOS was used to calculate the volume swelling to compensate the buoyancy effects and therefore determine the corrected solubility. Effects of parameters such as pressure, temperature, polymer and bowing agents were examined and discussed. It was observed that the branched molecular structure limited the molecular movement, and therefore the volume swelling of the polymer/gas mixture. The solubility of both N_2 and CO_2 were less in the branched polymer (ethene/octene copolymer) than in the linear PP.

References

1. Tong, J.; Moffitt, M.; Huang, X. J Polym Sci Part A: Polym Chem 2000, 39, 239.
2. Mehta, S.; Mirabella, F. M.; Rufener, K. J Appl Polym Sci 2004, 92, 928.
3. Lu, J.; Wei, G.; Sue, H. J Appl Polym Sci 2000, 76, 311.
4. Shah, S.; Kakarala, N. SPE-ANTEC 2000, 58, 2638.
5. Naguib, H. E.; Park, C. B.; Panzer, U. Polym Eng Sci 2002, 42, 1481.
6. Klempner, D.; Frisch, K. C. Handbook of Polymeric Foams and Foam Technology; Oxford University Press: Munich, 1991.
7. Frisch, K. C.; Saunders, J. H. Plastics Foams; Marcel Dekker: New York, 1972.
8. Park, C. B.; Suh, N. P. Polym Eng Sci 1996, 36, 34.
9. Throne, J. Thermoplastic Foam Extrusion; Hanser Gardner: Cincinnati, OH, 2004.
10. Han, J. H.; Han, C. D. J Polym Sci Part B: Polym Phys 1990, 28, 743.
11. Han, J. H.; Han, C. D. J Polym Sci Part B: Polym Phys 1990, 28, 711.
12. Park, C. B.; Baldwin, D. F.; Suh, N. P. Polym Eng Sci 1995, 35, 432.
13. Park, C. B.; Behravesh, A. H.; Venter, R. D. ACS Symp Ser 1997, 669(Polymeric Foams), 115.

TABLE II
Parameters for Henry's Constant

Mixture	H_0 (g-gas/ (g-polymer*psi))	E_a (J/mol)
PP + N_2	4.333×10^{-5}	5648.5
PP + CO_2	1.812×10^{-5}	−4749.8
Ethene/octene copolymer + N_2	1.491×10^{-5}	2768.3
Ethene/octene copolymer + CO_2	1.134×10^{-5}	−5652.0

14. Park, C. B.; Cheung, L. K. Polym Eng Sci 1997, 37, 1.
15. Sato, Y.; Yurugi, M.; Fujiwara, K. Fluid Phase Equilib 1996, 125, 129.
16. Sato, Y.; Fujiwara, K.; Takikawa, T. Fluid Phase Equilib 1999, 162, 261.
17. Sato, Y.; Takikawa, T.; Takishima, S. J Supercritical Fluids 2001, 19, 187.
18. Sato, Y.; Takikawa, T.; Yamane, M. Fluid Phase Equilib 2002, 194, 847.
19. Sato, Y.; Takikawa, T.; Sorakubo, A. Ind Eng Chem Res 2000, 39, 4813.
20. Areerat, S.; Hayata, Y.; Katsumoto, R.; Kegasawa, T.; Egami, H.; Ohshima, M. J Appl Polym Sci 2002, 86, 282.
21. Wong, B.; Zhang, Z.; Handa, Y. P. J Polym Sci Part B: Polym Phys 1998, 36, 2025.
22. Li, G.; Wang, J.; Park, C. B.; Moulinie, P.; Simha, R. SPE-ANTEC 2004, 62, 2566.
23. Sanchez, I. C.; Lacombe, R. H. J Polym Sci Polym Lett Ed 1977, 15, 71.
24. Sanchez, I. C.; Lacombe, R. H. Macromolecules 1978, 11, 1145.
25. Suhm, J.; Maier, R. D.; Kressler, J.; Muelhaupt, R. Acta Polymerica 1998, 49, 80.
26. Kleinrahm, R.; Wagner, W. J Chem Thermodyn 1986, 18, 739.
27. Li, G.; Wang, J.; Park, C. B.; Simha, R. In Advances in Plastic Components, Processes, and Technologies 2005; Society of Automotive Engineers: Warrendale, PA, 2005.